ELSEVIER

Journal of Molecular Catalysis A: Chemical 168 (2001) 247–256

JOURNAL OF MOLECULAR CATALYSIS A: CHEMICAL

www.elsevier.com/locate/molcata

A study of the surface acidity of acid-treated montmorillonite clay catalysts

U. Flessner [a], D.J. Jones [b,1], J. Rozière [b], J. Zajac [b], L. Storaro [c], M. Lenarda [c,*], M. Pavan [c], A. Jiménez-López [d], E. Rodríguez-Castellón [d,2], M. Trombetta [e], G. Busca [e,3]

[a] *Süd-Chemie AG, 85368 Moosburg, Germany*
[b] *Laboratoire des Agregats Moleculaires et Materiaux Inorganiques, UMR CNRS 5072, Université Montpellier II, 34095 Montpellier, France*
[c] *Dipartimento di Chimica, Università di Venezia Ca' Foscari, Dorsoduro, 2137-30123 Venezia, Italy*
[d] *Departamento de Quìmica Inorgánica, Cristalografia y Mineralogía, Universidad de Málaga, Apdo. 59, 29071 Málaga, Spain*
[e] *Dipartimento di Ingegneria Chimica e di Processo, Università, P. le J.F. Kennedy, I-16129 Genova, Italy*

Received 17 July 2000; accepted 24 October 2000

Abstract

The surface acidity of a series of commercial Süd Chemie acid-treated montmorillonite clays (K-catalysts) has been evaluated by a wide range of complementary experimental techniques. The different methods applied allow a rather complete characterisation of the surface acidity providing a complete picture of the Lewis/Brønsted acid strength/density of the surface sites. IR data show that the Brønsted sites on these catalysts are relatively weak and provide evidence for a slight increase of the strength and the density of Brønsted sites in the order K5 < K10 ∼ K20 < K30 in full agreement with the trend in *iso*-butene conversion, which is a measure of the strength and/or the abundancy of Brønsted sites. The apparent contradiction of these data with those obtained from the ammonia adsorption and *iso*-propanol conversion experiments can be explained by the structural and chemical modification of the clays upon acid treatment.

Keywords: Acid clays; K-catalysts; Acidity

1. Introduction

Solid acids find a wide range of catalytic applications in oil and chemical conversion processes [1–5]. The use of aluminosilicates in heterogeneous catalysis is almost old as the catalysis concept itself [6–9]. Among the earliest cracking catalysts were acid-activated bentonites and kaolinite clays, these being replaced in the 1960s by large pore Y-zeolites. The process by which natural calcium bentonites are acid-activated involves treatment of the uncalcined clay with mineral acids at 366 K of variable concentration and for different duration. Such treatment leads to leaching of aluminium, magnesium and iron cations from the octahedral layer, to partial removal of aluminium ions from the tetrahedral layer that relocate in the interlayer space, and to the reduction of cation exchange capacity by one-half. Non-negligible

* Corresponding author. Tel.: +39-41-2578567; fax: +39-41-2578517.
E-mail addresses: debtoja@univmontp2.fr (D.J. Jones), lenarda@unive.it (M. Lenarda), castellon@ccuma.sci.uma.es (E. Rodríguez-Castellón), icibusca@csita.unige.it (G. Busca).
[1] Fax: +33-4671-43304.
[2] Fax: +34-9521-32000.
[3] Fax: +39-10-3536028.

1381-1169/01/$ – see front matter
PII: S1381-1169(00)00540-9

physical changes also take place during acid activation: swelling occurs at the edges of clay platelets which open up and separate, while still remaining tightly stacked at the centre. The surface area increases notably, and pore diameters increase and assume a three-dimensional form. Different grades of acid-activated montmorillonites are tailored to different applications. Acid-treated montmorillonites can be purchased from a variety of commercial sources. The acid-treated clay K10 is produced by Süd Chemie AG of Moosburg, Bavaria (Germany), and has been obtainable from Fluka AG and Aldrich Chemical Co. for a number of years. The ease of availability explains why synthetic organic chemists have largely used this material in a wide range of acid catalysed reactions. In spite of its wide use, and despite several studies on acid treatments of clays [10–16], the nature of the acid sites and the details of the surface chemistry of these versatile catalytic materials is still in part unknown.

We report here an evaluation of the surface acidity of the well known K10 and of some other acid-activated clays of the K-series (K5, K20, K30) using a range of complementary experimental techniques.

2. Experimental

2.1. Materials

K-montmorillonites are produced by Süd Chemie AG from raw clays of Bavaria, Germany, and laboratory quantities are commercially available from Fluka. Acid activation is performed for a variable length of time, with HCl of variable concentration at boiling temperature, using corporate technology. Surface areas (BET) and pore distribution (BJH) were measured with a Micromeritics ASAP 2010 apparatus.

2.2. Ammonia chemisorption

The amounts of NH_3 adsorbed at different partial pressures in the equilibrium bulk phase were measured using a Micromeritics ASAP 2010 Chemi System apparatus. In order to reduce physisorption of ammonia on the solid surface, the adsorption temperature was maintained at 353 K. Prior to adsorption measurements, the solid sample (about 200 mg) was outgassed at 723 K for 3 h. Successive ammonia doses were sent onto the sample until a final equilibrium pressure of 38 Torr was reached. The equilibrium pressure was measured after every adsorption step, and the amount adsorbed was calculated. At the end of the first adsorption cycle, the sample was pumped at 353 K for 30 min, and a second adsorption cycle was then performed at the same temperature. The difference in adsorption between two adsorption cycles is ascribed to irreversible adsorption of NH_3 on surface of the K-catalyst. At first, this quantity changes as the adsorption progresses, but then it levels-off. Similar behaviour is observed for all four K-catalyst samples.

2.3. Iso-propanol decomposition

The catalytic activity of the samples in the decomposition of *iso*-propanol was tested in a fixed bed tubular glass microreactor at 623 K and atmospheric pressure using about 30 mg of catalyst with dilution. The *iso*-propanol was fed into the reactor by bubbling a flow of He through a saturator–condenser at 303 K, which allowed a constant flow of 25 ml min^{-1} with 7.4% of *iso*-propanol and space velocity of 41 mol g^{-1} s^{-1}. The samples were pretreated at 493 K in He flow for 2 h and then kept 1 h at 493 K under static He atmosphere. The gas carrier was passed through a molecular sieve trap before being saturated with *iso*-propanol. The reaction products were analysed by on-line gas chromatograph provided with a flame ionisation detector and a fused silica capillary column SPB1.

2.4. Microcalorimetric measurements of the enthalpy of competitive adsorption of 1-butanol

The experimental procedure is based on the flow calorimetric titration of the hydrophilic sites with 1-butanol as a hydrophilic probe. In order to eliminate a van der Waals–Lifshitz contribution to the enthalpy of displacement, the titrant is used in an apolar solvent (*n*-heptane). The enthalpy changes accompanying the adsorption of 1-butanol from *n*-heptane at 298.15 K were determined using a Microscal Flow Microcalorimeter [17,18]. For all calorimetric measurements, solid samples were taken at random and sieved to obtain 40–400 μm diameter fractions. The flow cell was filled with a mixture of about 20 mg of a K-catalyst sample and PTFE powder. The latter is

a solid diluent, used to shorten the time of adsorption. The dry adsorbent in the cell was evacuated to 0.1 mmHg for 2 days at room temperature, and then wetted with *n*-heptane and additionally purified by solvent percolation at a rate of $3\,ml\,h^{-1}$ for 1 h. After attaining thermal equilibrium, the flow of the solvent was exchanged for that of a $2\,g\,l^{-1}$ solution of 1-butanol in *n*-heptane. The displacement of the solvent by the adsorbing solute molecules on hydrophilic surface sites induces a thermal effect and alters the thermal equilibrium which is recorded by the thermistors as a thermal peak, the area under the peak being proportional to the total heat evolved. A calibration coil in the cell allows correlation between a fixed energy supplied and the integrated value recorded. The formation of adsorbate monolayers on the solid surface is indicated by an on-line refractive index detector, which continuously monitors differences between the refractive index of the solution passing through the adsorbent bed and that of the pure solvent.

2.5. Catalytic isomerisation of 1-butene

Catalytic 1-butene isomerisation tests were performed in a tubular glass flow microreactor. The catalyst samples were pretreated for 2 h in N_2 flow at 673 K. Experiments were performed at 673 K and $\tau = 2.4\,g_{(cat)}\,g_{(1\text{-butene})}{}^{-1}\,h$. The 1-butene was at 5% abundance in nitrogen. Any non-converted 1-butene and the reaction products were analysed on line in a gas chromatograph (HP 5890 series II) equipped with a wide-bore $KCl/AlCl_3$ column ($\varnothing = 0.53\,mm$, $l = 50\,m$) and a flame ionisation detector. As usual for this reaction, the distribution of *n*-butenes is near equilibrium, and consequently, the conversion is defined as the ratio (products — *n*-butenes)/1-butene feed × 100. Selectivity was calculated as $S_L = 100 \times (\text{wt.\% } iso\text{-butene})_{effluent}/[(\text{wt.\% } n\text{-butenes})_{feed} - (\text{wt.\% } n\text{-butenes})_{effluent}]$. The amount of coke was deduced from the weight loss of the spent catalyst after burning in air in the range 363–1073 K, as measured by thermogravimetry (TG).

2.6. FT-IR spectra in the OH stretching region before and after adsorption of a probe (pivalonitrile) for basic sites

Infrared (IR) spectra were recorded on a Nicolet Magna 750 instrument with a resolution of $4\,cm^{-1}$. Self-supported pressed disks (ca. $8\,mg\,cm^{-2}$) were activated in the IR cell by heating under vacuum (10^{-4} Torr) at the corresponding calcination temperature for 2 h. Pivalonitrile (1 Torr at equilibrium) was introduced at room temperature, then immediately evacuated at the same temperature to eliminate physisorbed species. Stepwise desorption was continued up to 573 K. A background spectrum was automatically subtracted each time.

3. Results

3.1. Analytical and structural data

Analytical and structural data are reported in Tables 1 and 2, respectively.

3.2. Determination of surface hydrophilic sites using competitive adsorption of 1-butanol (BuOH) from a liquid phase at 298 K

The integral enthalpy of displacement per unit BET surface area is a measure of the number of the hydrophilic surface sites detected by the butanol probe

Table 1
Apparent bulk density, surface area and pore volume distribution of K-catalysts

Sample	Apparent bulk density ($g\,l^{-1}$)	Surface area BET ($m^2\,g^{-1}$)	Pore volume ($ml\,g^{-1}$)		
			0–80 nm	0–24 nm	0–14 nm
K5	600	200	0.25	0.22	0.18
K10	370	240	0.36	0.30	0.26
K20	470	240	0.39	0.32	0.30
K30	450	330	0.50	0.44	0.38

Table 2
Chemical analysis of K-catalysts

Sample	Chemical analysis (%)								
	SiO_2	Al_2O_3	Fe_2O_3	CaO	MgO	Na_2O	K_2O	Loss on ignition	Total
K5	65.0	19.0	4.8	0.2	2.4	0.3	1.5	6.5	99.7
K10	73.0	14.0	2.7	0.2	1.1	0.6	1.9	6.0	99.5
K20	75.0	12.5	2.4	0.3	1.2	0.3	1.5	6.3	99.5
K30	80.0	10.0	1.8	0.2	1.0	0.3	0.5	6.0	99.8

under given experimental conditions [19]. In the second stage, the partial desorption of butanol is achieved by exchanging the flow of the solution for that of pure *n*-heptane. The desorption cycle is carried out to evaluate the extent of adsorption reversibility. Partial reversibility of 1-butanol adsorption indicates the existence of very strong hydrophilic sites in the sample surface at which the alcohol molecules are irreversibly localised during the displacement process. The results on the four K-catalyst samples are given in Table 3.

A direct comparison of the surface hydrophilic character between the four K-catalysts is possible because they are expected to have similar surface chemistry. K20 clearly possesses the greatest number of hydrophilic sites per unit surface area. About 50% of these sites interact with the butanol molecules so strongly that the adsorption is irreversible. For the remaining samples, the density of hydrophilic sites is fairly similar, with K10 giving the highest degree of irreversibility. Therefore, the hydrophilic character of the surface, as measured by the competitive 1-butanol adsorption from *n*-heptane, decreases in the following order: K20 > K10 ≈ K5 ≈ K30.

A marked degree of the adsorption irreversibility indicates that the surface of the samples is heterogeneous in regard to the strength of interactions between the BuOH molecules and hydrophilic sites.

Table 3
Thermal effects in the first adsorption–desorption cycle of BuOH onto K-catalysts from a $2\,g\,l^{-1}$ *n*-heptane solution at 298 K

Sample	S_{BET} ($m^2\,g^{-1}$)	ΔH_{ads} ($mJ\,m^{-2}$)	ΔH_{des} ($mJ\,m^{-2}$)	$\Delta H_{des}/\Delta H_{ads}$ (%)
K5	200	29.8	25.0	84
K10	240	31.7	12.1	38
K20	240	50.5	26.4	52
K30	330	28.6	17.7	62

3.3. Evaluation of the number of acid sites

3.3.1. Two-cycle adsorption of NH_3 from a gaseous phase at 298 K

The chemisorption of ammonia from the gas phase is a powerful method of determining the number of acid sites of a solid surface. The acidity evaluation of MCM-41 type materials by this methodology has been reported recently [20]. The difference in adsorption of the two adsorption cycles at a pressure of 38 Torr corresponds to the maximum amount of NH_3 irreversibly adsorbed on the surface of the acid-activated clays. Since, irreversible adsorption of NH_3 means the localised chemisorption of single ammonia molecules on acidic sites, this quantity provides the total number of acidic sites on a solid surface. The numbers of surface acidic sites on the K-catalysts are given in Table 4.

Of the four K-catalyst samples used in the study, K5 possesses the greatest number of acidic sites per unit surface area of adsorbent. The order of decreasing number of acidic sites in the series is K5 > K10 ∼ K20 > K30.

Table 4
Number of surface acidic sites on K-catalysts as determined from the measurements of the adsorption of gaseous NH_3 at 353 K and $P = 38$ Torr

Sample	S_{BET} ($m^2\,g^{-1}$)	Number of sites ($mmol\,g^{-1}$)	Number of sites ($\mu mol\,m^{-2}$)
K5	200	0.27	1.35
K10	240	0.20	0.83
K20	240	0.19	0.79
K30	330	0.18	0.55

Table 5
Catalytic decomposition of *iso*-propanol to propene

Sample	*Iso*-propanol decomposition	
	$\mu mol_{(propene)}$ ($g^{-1}\,s^{-1}$)	$\mu mol_{(propene)}$ ($m^{-2}\,s^{-1}$)
K5	22.4	0.11
K10	23.4	0.10
K20	21.8	0.09
K30	18.6	0.06

3.3.2. Catalytic decomposition of iso-propanol to propene

The conversion of *iso*-propanol is a widely used reaction to test the acid–base and redox properties of catalysts. The reaction, that does not need strong acid sites, can give diisopropyl ether, propene and acetone as products. Propene is produced by simply acid-catalysed dehydration, while ether formation must involve an intermolecular coupling reaction. Acetone is formed in presence of basic or redox sites via oxidative dehydrogenation. For the K-montmorillonites, the selectivity to propene was found to be 100%. The data for all the samples are summarised in Table 5.

Neither the above technique nor ammonia chemisorption discriminates between Brønsted and Lewis acid centres, and the results given by these approaches can be compared. Fig. 1 shows the activity of the four K-catalysts in the decomposition of *iso*-propanol, and the number of surface acid sites as determined by ammonia adsorption, both expressed per unit surface area. It may be seen that the decrease in the decomposition of *iso*-propanol parallels the total number of acid sites.

3.3.3. Catalytic activity in 1-butene isomerisation

The skeletal isomerisation of 1-butene is an acid-catalysed reaction and it can be a useful test to compare the acidity of clay catalysts [21,22]. The conversion and the selectivity of the reaction considerably depend on the concentration, type and strength of the acid sites. Further, the distribution of some of the reaction products, in particular *iso*-butene, *n*- and *iso*-butanes and coke is strongly related to the strength and the type of the acid sites of the catalyst.

Dimerisation and oligomerisation products are formed when porous materials are used as catalysts. The most important by-products of isomerisation of 1-butene are the C3 and C5 alkenes derived from cracking degradation of C8 dimeric species. On the other hand, aromatics and carbonaceous compounds originate from oligomerisation followed by cracking and consequent coke deposition. A high concentration of very strong acid sites is responsible for the coke

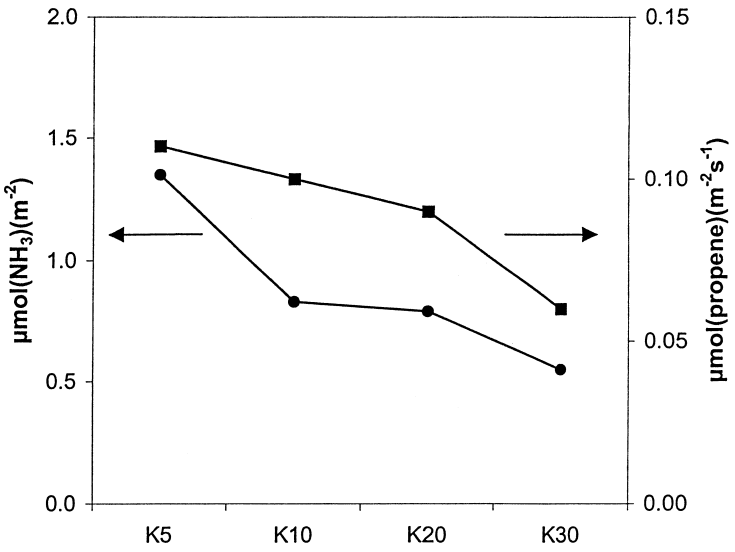

Fig. 1. Catalytic decomposition of *iso*-propanol to propene (■), and number of surface acidic sites (●) as determined by NH_3 adsorption on K-catalysts.

Table 6
Product distribution of 1-butene isomerisation on K-catalysts[a]

Sample	C3	Product distribution (%)				
		Iso-butane	*n*-Butane	*Iso*-butene	*n*-Butene	C5
K5	0.7	0.1	0.1	7.1	91.2	0.7
K10	0.4	0.0	0.1	5.0	93.6	0.5
K20	0.5	0.1	0.1	6.0	91.9	0.4
K30	0.5	0.1	0.1	6.6	90.4	0.4

[a] Conditions: $T = 673\,K$, $\tau = 6.4$, time on stream $= 2\,h$; increasing amount of >C5 compounds were observed going from K5 to K30. Coke formation was always negligible.

Table 7
Conversion, selectivity to *iso*-butene, and total amount of the skeletal isomerisation products on the K-catalysts

Sample	1-Butene isomerisation		
	Conversion (%)	S_L	Iso_{total}
K5	8.8	80.2	7.2
K10	6.4	78.4	5.0
K20	8.1	74.8	6.1
K30	9.6	68.8	6.7

deposits. The distribution of all these products is also influenced by the type of porosity of the catalyst.

The reaction products distribution, the conversion and selectivity to *iso*-butene are compiled in Tables 6 and 7. The total amount of skeletal isomerisation products (Table 7) was calculated by adding the amount of *iso*-butene to that of *iso*-butane, assuming that the latter originates from the former.

After 120 min of time-on-stream (TOS), conversion is less then 10% for all the samples, but the selectivity to *iso*-butene is quite high. Coke formation was always negligible, and only a very small amount of cracking products (C3 and C5) were detected. The trends of the conversion, selectivity and yield in skeletal isomerisation products of 1-butene with increasing TOS are shown in Figs. 2–4.

The conversion of 1-butene decreases with time while the selectivity remains almost constant. A slight increase during the first hour of reaction of the selectivity to *iso*-butene was found only for the K5 sample (Fig. 3). This is probably due to the presence on K5 of some very strong acid sites that are deactivated by coking within the first few minutes of reaction. These sites may also be responsible for the higher amount of skeletal isomerisation (*iso*-total) products detected in the first few minutes of the reaction. In contrast, the formation of *iso*-products follows the same trend for all the samples (Fig. 4).

Both *n*-butene conversion and the yield in *iso*-butene decrease in the order K30 > K20 > K10. The *iso*-butene selectivity, S_L, was found to decrease in the order K5 > K10 > K20 > K30 reflecting the gradual occurrence of bimolecular reactions leading to >C6 compounds as the BET surface area increases (Tables 1 and 2). The sample K5, which has the lowest BET area, gives the highest amount of *iso*-products and has the highest conversion for short TOS.

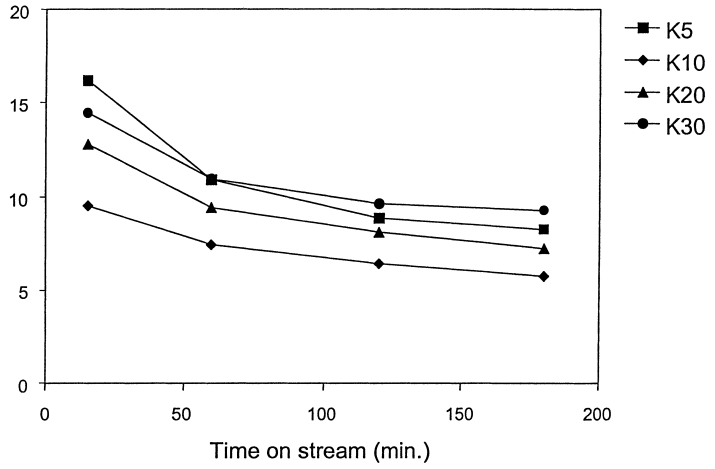

Fig. 2. Conversion (%) of 1-butene at increasing time-on-stream on K-catalysts.

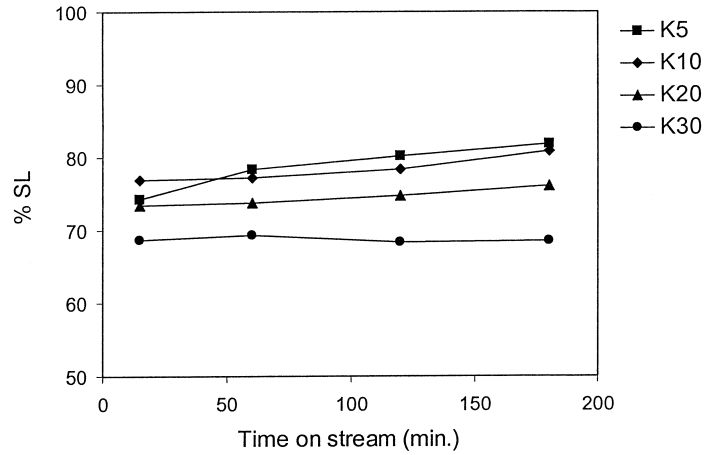

Fig. 3. Selectivity of K-catalysts in skeletal isomerisation products at increasing time-on-stream.

3.3.4. FT-IR study: surface hydroxy-groups and adsorption of pivalonitrile as a probe for surface acidity

3.3.4.1. Surface hydroxy-groups. The IR spectra in the OH stretching region after outgassing at 773 K of the montmorillonite samples are reported in Fig. 5. All samples show two main bands centred at 3742 and near 3640 cm^{-1} (Table 8). The band near 3742 cm^{-1} is due to silanol groups (Si–OH) exposed at the external layer surface in defect sites, while the broader band centred near 3640 cm^{-1} is due to Al_2OH groups in the interlayer region. The relative intensities of these two bands, expressed as the intensity ratio "band of silanol species/band of interlayer Al–OH" has its maximum for the sample with the highest Si/Al ratio (Table 8, K30 sample), and conversely, its minimum for the sample with the lowest Si/Al ratio (K5). As for the two samples with intermediate Si/Al ratio (K10 and K20), a similar intermediate value of this ratio is found. On the other hand, the surface areas of these samples also show a similar trend, being maximum for the sample K30, minimum for K5 and intermediate and similar for K10 and K20. This is a support for

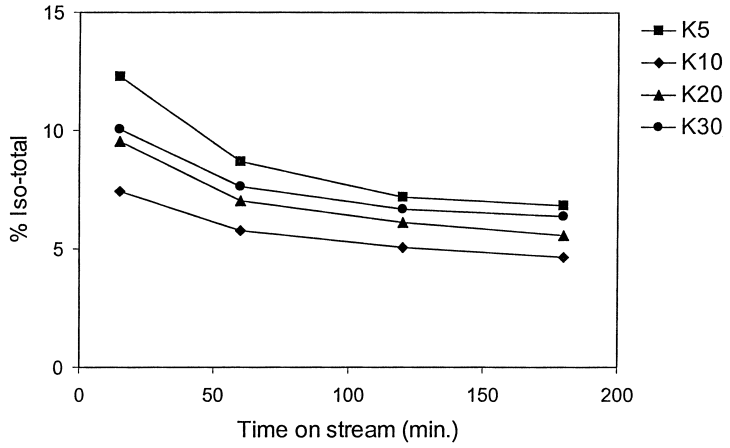

Fig. 4. Total isomerisation products (*iso*-butene + *iso*-butane) formed on K-catalysts at increasing time-on-stream.

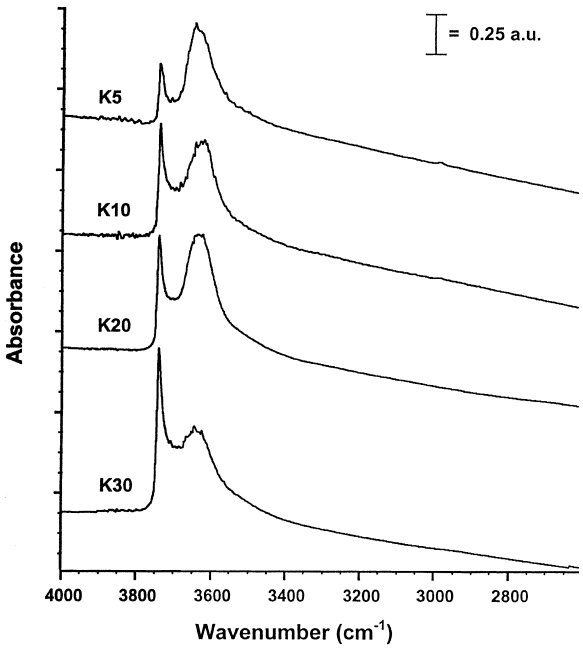

Fig. 5. FT-IR spectra of the K-catalysts in the 4000–2000 cm^{-1} area.

assignment to external silanol groups for the band at 3742 cm^{-1}. On the other hand, we can measure that the silanol band actually increases by the factor of 2.84 (in absolute terms), while the surface area only increases of a factor of 1.65, suggesting that the acid treatment also frees silanol groups in flat surfaces.

3.3.4.2. Adsorption of pivalonitrile (PN) as a probe for surface acidity. The IR spectra of the K-samples upon adsorption and desorption of PN are reported in the OH stretching region and CN stretching region in Fig. 6A and B, respectively. It is seen in all cases that upon adsorption of PN, the OH band at 3742 cm^{-1} disappears, while the band near 3640 cm^{-1} is not affected (or only in part involved). The $\Delta\nu$OH and νCN due to PN adsorption on the catalysts are reported in Table 8. The $\Delta\nu$OH is found in all cases, in the range 310–325 cm^{-1}. This indicates that the predominant sites are medium-weak Brønsted sites, but the absolute intensity of the perturbed band follows the intensity of the unperturbed band at 3742 cm^{-1}, i.e. it follows the trend K30 $\gg$ K20 $\approx$ K10 $\gg$ K5. This is an indication of a decrease in the Brønsted acid site density (number of acid sites per unit mass of solid) in this order. On the other hand, the position of the maximum of the OH band, when perturbed by PN, shifts slightly but significantly in the order K5 $<$ K10 $\sim$ K20 $<$ K30. This suggests that the Brønsted sites of K30 are a little more acidic than that of the other samples.

In the CN stretching region, all samples show the same features. They show four main bands, the two of which at higher frequencies are assigned to two different H-bonded species over non-acidic and weakly acidic OHs, while the two components at lower frequencies can be assigned to species adsorbed on two different families of Lewis acid sites. In particular, the band at about 2300 cm^{-1} is due to species interacting with very strong Lewis sites, probably Al^{3+} in partly unsaturated tetrahedral coordination, like those of transitional alumina. The band near 2270 cm^{-1} could be due to Al^{3+} with partly unsaturated octahedral coordination. In Table 8, the ratio of the intensity of the silanol band (measured on the activated samples) and of the CN stretching band (measured on the samples outgassed at 373 K after PN adsorption) shows a continuous decrease in the order K5 $>$ K10 $\sim$ K20 $>$ K30. This shows that the ratio between Lewis and Brønsted acid sites is more in favour of Lewis sites for K5 and shift towards Brønsted sites for K30.

Table 8
FT-IR spectroscopic data on K-catalysts

Samples	Si/Al	νOH (activity) (cm^{-1})	$\Delta\nu$OH (PN)	νCN (PN) (cm^{-1})				νCN/νOH
				I	II	III	IV	
K5	7	3742, 3640	312	2305	2269	2250	2235	0.16
K10	10	3742, 3630	315	2305	2270	2250	2235	0.11
K20	12	3742, 3635	315	2305	2270	2250	2235	0.11
K30	16	3742, 3645	322	2300	2270	2250	2235	0.06

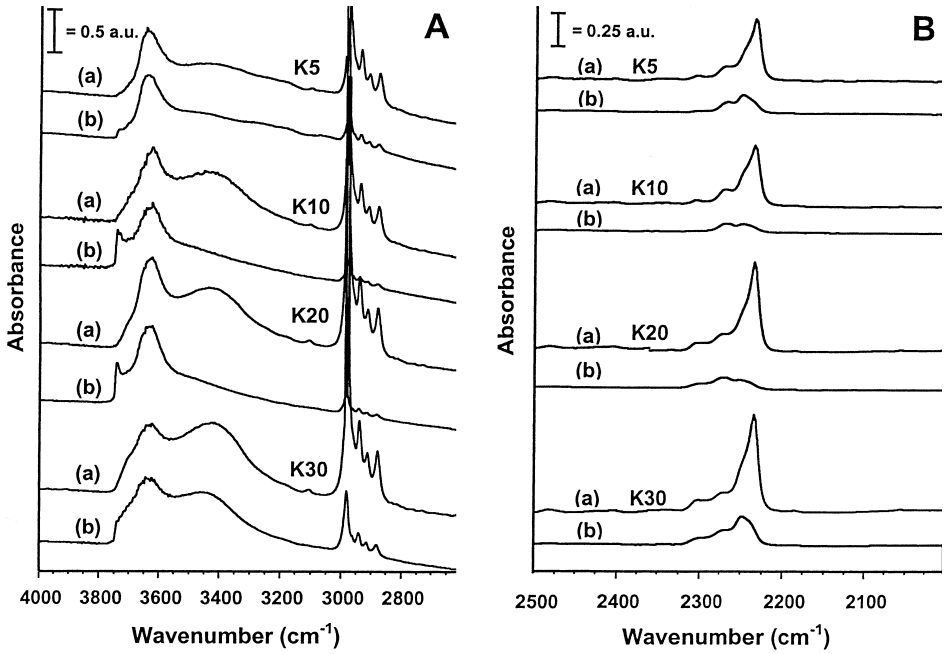

Fig. 6. FT-IR spectra of K-catalysts upon adsorption and desorption of pivalonitrile (PN) in the 4000–2000 cm^{-1} (A) and 2500–2000 cm^{-1} (B) area.

3.4. Discussion and conclusions

The acid-treated montmorillonites denoted as K-clays are commercial Süd Chemie products that have found wide application as heterogeneous catalysts for several important reactions both on industrial and laboratory scales [8,23,24]. In the present paper, we have reported the results of the characterisation of the surface acid properties of these materials using a broad range of complementary techniques.

The different methods applied allow a rather complete picture of the surface structure of these materials to be drawn. The results from the adsorption of ammonia and the catalytic activity in both *iso*-propanol decomposition and *n*-butene conversion point to the significant surface acidity of these samples but also show that the different samples have a different distribution of Lewis and Brønsted sites. IR spectroscopy allows characterisation of the surface Brønsted acidity as due to terminal silanols, located at the external surface of the "tetrahedral" layers. Previous studies [21,22] have shown that Brønsted sites are mainly responsible for catalytic activity in *n*-butene conversion. IR data show that the Brønsted sites on these catalysts are in fact relatively weak, and provide evidence for a slight increase of the strength and the density of Brønsted sites in the order K5 < K10 ∼ K20 < K30. This fully agrees with the trend in *iso*-butene conversion which is a measure of the strength and/or the abundancy of Brønsted sites. This also agrees with the inverse trend observed for the selectivity to *iso*-butene which is generally found to be higher, the weaker the Brønsted acidity of the catalysts.

The data concerning ammonia adsorption and *iso*-butene conversion show quite an opposite trend. In fact, the K5 sample is the most active in producing propene from *iso*-propanol and in adsorbing ammonia. Previous studies showed that Lewis sites are generally involved in alcohol dehydration, while ammonia can adsorb both on Lewis and Brønsted sites.

IR spectroscopy clearly shows that strong Lewis sites are observed in all cases due to Al^{3+} ions in low coordination. The IR data also support the idea that acid treatment causes a loss of Lewis acid sites. This is probably due to the partial dissolution of the octahedral layer in acid solution which results in exposure

of the tetrahedral layers. Thus, the IR data fully account for the higher activity of K5 in adsorbing ammonia and converting *iso*-propanol, and on these bases also for the trend observed during the experiments of competitive adsorption of 1-butanol. Since alcohols can adsorb both on Lewis and on Brønsted sites, and since the densities of such sites have opposite trends with respect to the acid treatment, the highest hydrophilic character is found for K20.

The data presented above agree with the chemistry of the acid treatment, which is known to cause the progressive dealumination and degradation of the octahedral clay layers [10–16]. This causes a reduction of the interlayer charge that results in a progressive opening of the edge of the clay layers making available the internal protonic acid sites to incoming molecules.

In the early stage of the acid attack, partial degradation of the octahedral layer and the substitution of Na^+ and the Ca^{2+}, naturally present as interlamellar cations, with the H^+ and/or the lattice ions (e.g. Al^{3+}) gives a material with low surface area (Table 1) and porosity. Further acid treatment causes a gradual increase of the surface area and of the pore diameters following the more extensive degradation of the octahedral layer, resulting in an increase in the amount of Brønsted acid sites and a decrease of the Lewis sites. As shown by NH_3 adsorption, *iso*-propanol decomposition and 1-butene isomerisation tests, the K5 sample appears to have the highest total number of acid sites, both Brønsted and Lewis, per solid mass unit. K10 and K20 show a very similar acidity of medium strength and similar developed mesoporosity, although still with a certain degree of layered structure retained. Finally, K30 seems to have the highest density of relatively stronger Brønsted acid as shown by FT-IR experiments and 1-butene isomerisation, but a very low component of Lewis acid sites due to the extensive loss of Al.

The data presented here also demonstrate that the careful analysis of different techniques aimed at the characterisation of the surface acidity provides a complete picture of the Lewis/Brønsted acid strength/density of the surface sites.

Acknowledgements

Financial support under Brite-EuRam contract BRPR-CT97-0560 is gratefully acknowledged.

References

[1] A. Corma, Chem. Rev. 95 (1995) 559.
[2] A. Corma, H. Garcia, Catal. Today 38 (1997) 257.
[3] H.J. Clark, D.J. Macquarrie, Org. Proc. Res. Dev. 1 (1997) 149.
[4] H.J. Clark, D.J. Macquarrie, Chem. Soc. Rev. 25 (1996) 303.
[5] K. Tanabe, W.F. Holderich, Appl. Catal. A 181 (1999) 399.
[6] P. Laszlo, Acc. Chem. Res. 19 (1986) 121.
[7] T.M. Adams, Appl. Clay Sci. 2 (1987) 309.
[8] J.A. Ballantine, in: K. Smith (Ed.), Solid Supports and Catalysts in Organic Synthesis, Harwood, UK, 1992, p. 100.
[9] M. Campanati, A. Vaccari, in: R. Sheldon, H. van Bekkum (Eds.), Fine Chemicals Through Heterogeneous Catalysis, VCH, Vienheim, 2000, pp. 61–79.
[10] C.R. Theocharis, K.J. s'Jacob, A.C. Gray, J. Chem. Soc., Faraday Trans. I 84 (1988) 1509.
[11] C. Pesquera, F. Gonzàlez, I. Benito, C. Blanco, S. Mendioroz, J. Pajares, J. Mater. Chem. 2 (1992) 907.
[12] C.N. Rhodes, D.R. Brown, J. Chem. Soc., Faraday Trans. 89 (1993) 1387.
[13] H. Kaviratna, T.J. Pinnavaia, Clays Clay Min. 42 (1994) 717.
[14] M.A. Vicente, M. Suarez, J. Lòpez-Gònzàlez, M.A. Bañares-Muñoz, Langmuir 12 (1966) 566.
[15] C. Breen, F.D. Zahoor, J. Madejová, P. Komadel, J. Phys. Chem. B 101 (1997) 5324.
[16] D. Haffad, A. Chambellan, J.C. Lavalley, Catal. Lett. 54 (1998) 227.
[17] J. Groszek, S. Partyka, Langmuir 9 (1993) 2721.
[18] J. Zajac, A.J. Groszek, Carbon 35 (1997) 1053.
[19] M.J. Meziani, J. Zajac, D.J. Jones, J. Rozière, S. Partyka, Langmuir 13 (1997) 5409.
[20] M.J. Meziani, J. Zajac, D.J. Jones, S. Partyka, J. Rozière, A. Auroux, Langmuir 16 (2000) 2262.
[21] M. Trombetta, G. Busca, M. Lenarda, L. Storaro, M. Pavan, Appl. Catal. A 182 (2) (1999) 225.
[22] M. Trombetta, G. Busca, M. Lenarda, L. Storaro, R. Ganzerla, L. Piovesan, A. Jimenez Lopez, M. Alcantara-Rodrìguez, R. Rodrìguez-Castellón, Appl. Catal. A 193 (2000) 55.
[23] D.R. Brown, Geol. Carpathica Series Clays 1 (1994) 45.
[24] R.W. Mc Cabe, in: D.W. Bruce, D. O'Hare (Eds.), Inorganic Materials, Wiley, New York, 1992, p. 296.